JACS Hosting Innovations

Contents List available at JACS Directory

# Journal of Advanced Chemical Sciences

journal homepage: www.jacsdirectory.com/jacs



# Variation of Surface Morphology and Physico-Chemical Properties of the Fly Ash Through Mechanical and Thermal Activations

A. Sharma<sup>1</sup>, S. Kabra<sup>2</sup>, S. Katara<sup>2</sup>, A. Rani<sup>2,\*</sup>

<sup>1</sup>Department of Chemistry, S.S. Jain Subodh P.G. (Autonomous) College, Rambagh Circle, Jaipur – 302 004, Rajasthan, India. <sup>2</sup>Department of Pure and Applied Chemistry, University of Kota, Kota – 324 005, Rajasthan, India.

#### ARTICLE DETAILS

Article history: Received 03 March 2015 Accepted 11 March 2015 Available online 16 March 2015

Keywords: Fly Ash Mechanical Activation Chemical Activation Acid Treatment Deposition-Precipitation Method Ball Milling

#### ABSTRACT

This article is a critical overview on the experimental results on development of activation techniques to acquire a deeper understanding of surface chemistry and to improve the catalytic activity of coal fly ash, in relation to its use as solid acid catalyst and catalytic support materials. Studied fly ash was collected from Jamshedpur Thermal Power Station as an extremely fine ash, formed from the inorganic components of the coal, mainly silica and alumina which remain after combustion of the carbonaceous part of the coal. Mechanical activation results in slight increase in silica percentage, amorphous nature, specific surface area and surface roughness, as evident by analytical measurements using XRF, XRD, FT-IR, BET surface area, TGA-DTA and SEM techniques. Thermal activation evaluates the changes in phase mineralogy, removal of amorphous carbon and enhanced the silica amount. The variation of surface and Physico-chemical properties of the fly ash by activation methods resulted in improved acid and therefore, catalytic activity of fly ash.

#### 1. Introduction

The coal fired power plant which consumes pulverized solid fuels composed of combustible organic matter with varying amount of inorganic mineral parts produce large amount of solid waste fly ash. Several billion metric tons of coal is mined per year throughout the world for use in combustion processes. During combustion of coal, beside energy, a variety of by-products are also produced such as fly ash, bottom ash and flue gas and desulfurization sludge [1]. Out of all the by-products fly ash is the major solid waste produced after the coal combustion. Fly ash is estimated to be produced up to 600 million tons per year in the world [2] and about 110 million tons in India [3]. Due to environmental regulations, new ways of utilizing fly ash have to be explored in order to safeguard the environment and provide cost effective ways for its bulk utilization. Now, there is an urgent need to adopt technologies for gainful utilization and safe management of FA on sustainable basis.

The mineral parts present in solid fuel coal include clay, micas, quartz, feldspars, sulphides, carbonates of iron, calcium, magnesium etc. During combustion, these minerals become fluid at high temperature and are then cooled. The combustible gasification takes place in furnace of coal fired boiler at an operative temperature 1450 °C (2500 F) under reducing atmosphere [4]. At these temperatures the mineral matter within the coal may oxidize, decompose, fuse, disintegrate and fly ash comes from small drops of melt and volatile compounds which are carried up by the ascending gases. The mixture of gases is cooled where fly ash gets solidify at temperature from 950 °C to 400 °C. Rapid cooling in the post combustion zone results in the formation of spherical particles known as fly ash consisting of silica, alumina, iron oxide, lime, magnesia and alkali in varying amounts with some unburned activated carbon [5-7] and possesses large surface area. Fly ash containing more than 70% SiO<sub>2</sub>, Al<sub>2</sub>O<sub>3</sub> and Fe<sub>2</sub>O<sub>3</sub> and less than about 5% CaO are classified as class F-fly ash and those containing higher CaO are referred to as class C-fly ash [8]. Higher SiO2 and Al2O3 of fly ash make it suitable to be used as solid catalyst and catalyst support for heterogeneous catalytic reactions important to industrial sectors. To improve activity of fly ash, several activation techniques such as mechanical and thermal activation are being used, proper activation techniques in order to increase its silica content and physico-chemical properties are being developed to vary its surface properties and converted into a catalyst as well as catalytic support material with similar catalytic activity as other solid acid catalysts derived from silica materials.

FA is transformed from micron sized to nano structured through high energy planetary ball milling [9]. The modification of morphology and size of FA experienced with milling confreres a great degree of reactivity to the FA as a catalyst or catalyst support material. Thermal activation evaluates the changes in phase mineralogy, removal of amorphous carbon and enhanced the silica amount.

The present work elaborates how to improve the capability of fly ash in order to increase its silica content and surface activity by mechanical activation and thermal treatments. In this paper an attempt has been made to modify the chemical, structural and morphological properties of FA through synergistic mechano-thermal activations.

## 2. Experimental Methods

#### 2.1 Materials

Class-F type fly ash having ( $SiO_2+Al_2O_3>80\%$ ) produced from combustion of bituminous coal, was collected from Tata Thermal Power Plant (TTPP) situated at Jamshedpur, Jharkhand. The components of fly ash are  $SiO_2$  (62%),  $Al_2O_3$  (23%),  $Fe_2O_3$  (7%), CaO (1.6%), MgO (0.8%),  $TiO_2$  (1.3%),  $Na_2O$  (2.8%) and trace elements (1.5%). The collected F-type fly ash sample has more than 70% of silica and alumina which makes fly ash, a suitable catalytic support material by various activation techniques.

#### 2.2 Activation Procedure

# 2.2.1 Mechanical Activation

The term 'mechanical activation' refers to enhanced reactivity of fly ash from combined effects of increased surface area and physicochemical changes induced in the bulk as well as on the surface.

Several techniques, under the broad classification of mechanical activation has been attempted to enhance the silica content and surfacial properties of fly ash. For this purpose the fly ash is mechanically activated using high energy planetary ball mill. Various methods for mechanical

\*Corresponding Author

Email Address: ashu.uok@gmail.com (A. Rani)

activation are as: Prolonged grinding [10, 11], micro-grinding or milling and sieving. All the three techniques have good effect and have its own advantages and disadvantages.

#### 2.2.1.1 Experimental Procedure

Fly ash was washed with distilled water followed by drying at 100 °C for 24 hr. Dried fly ash was mechanically activated using high energy planetary ball mill (Retsch PM-100, Germany) in an agate grinding jar using agate balls of 5 mm ball sizes for 5, 10 and 15 hours with 250 rpm rotation speed. The ball mill was loaded with ball to powder weight ratio (BPR) of 10:1. Mechanically activated fly ash was calcined at 900 °C for 4 hr for removing carbon, sulphur and other impurities before characterization.

#### 2.2.2 Thermal Activation

Thermal activation is a term given to any waste treatment technology that involves high temperatures in the processing of the waste feedstock. Thermal treatment reduces the volume and masses of the waste and inert the hazardous components. It is reported that low temperature calcinations (800-1000 °C, 80-150 minutes) of fly ash would change the chemical components and mineral structure when adding some mineralized agent. The thermal activation is generally done by following processes: Heat activation [12], hydrothermal processing [13] and dry curing [14]. During thermal treatment of fly ash, quartz is inherited and crystallization of mullite and corundum occurs. The mineral structure of most of the silico-aluminates collapses, leading to appearance of a vitreous phase [15]. During the thermal activation high temperature calcinations of fly ash is carried out in muffle furnace and thermally activated fly ash (TAFA) is analyzed for colour, mineralogical, structural, morphological and thermal properties.

#### 2.2.2.1 Experimental Procedure

As received fly ash was calcined from 500 °C, 700 °C, 900 °C in a thermocouple-controlled muffle furnace at a rate of 15 °C per minute to maximum temperatures of 500 °C, 700 °C, 900 °C with 1h holding time. At each interval, lose on ignition (LOI), colour and X-ray diffraction mineralogy were determined.

#### 2.3 Characterization Techniques

Fly ash samples before and after mechanical and thermal activations were analyzed by X-ray fluorescence spectrometer (Philips PW1606). The BET surface area was measured by  $N_2$  adsorption-desorption isotherm study at liquid nitrogen temperature (77 K) using Quanta chrome NOVA s1000e surface area analyzer. Powder X-ray diffraction studies were carried out by using (Philips X'pert) analytical diffractometer with monochromatic  $CuK_\alpha$  radiation (k = 1.54056 Å) in a 20 range of 0-80°. Crystallite size of the crystalline phase was determined from the peak of maximum intensity (20 = 26.57°) by using Scherrer formula [16] as Eq. (1) with a shape factor (K) of 0.9.

Crystallite size = 
$$K.\lambda / W.\cos\theta.....(1)$$

Where, W=Wb-Ws; Wb is the broadened profile width of experimental sample and Ws is the standard profile width of reference silicon sample. The FT-IR study of the samples was done using FT-IR spectrophotometer (Tensor-27, Bruker, Germany) in DRS (Diffuse Reflectance Spectroscopy) system by mixing the sample with KBr in 1:20 weight ratio. The detailed imaging information about the morphology and surface texture of the sample was provided by SEM (Philips XL30 ESEM TMP).

#### 3. Results and Discussion

## 3.1 Chemical Composition

The chemical composition of as received fly ash (FA), mechanically activated (MFA) fly ash samples milled for 5, 10 and 15h, and thermally activated fly ash (TAFA) samples at various activated temperatures and durations as analyzed by XRF are given in Table 1 and Table 2. Fly ash sample contained high SiO<sub>2</sub>, Al<sub>2</sub>O<sub>3</sub>, Fe<sub>2</sub>O<sub>3</sub> as major percentage and other inorganic oxides are present in low %. Variation in composition of metallic oxides with milling time can be observed in Table 1, which indicates that percentage of alumina reduces marginally and the percentage of silica increases marginally on increasing milling time from 5h to 15h [17,18] and there after it remains unaffected with milling time. TiO<sub>2</sub> percent decreases and those of CaO and Fe<sub>2</sub>O<sub>3</sub> marginally increase with long hours of milling [9].

The thermal activation increased the silica amount greatly (61.9% to 70%). The variation in silica composition of FA at different temperature

indicates that the silica percentage is increased marginally at  $500\,^{\circ}\text{C}$  to  $700\,^{\circ}\text{C}$  but greatly after heating at  $900\,^{\circ}\text{C}$  for 4h. Thermal activation of fly ash removes mainly unburnt carbon and moisture besides few metals and sulphur content resulting in increase in silica and alumina percentage.

**Table 1** Chemical composition of FA and MFA (5h, 10h, and 15h) determined by XRF technique

Chemical	FA	MFA			
components		5h	10h	15h	
SiO <sub>2</sub>	61.9	62.2	63	66	
Al <sub>2</sub> O <sub>3</sub>	29.7	29.6	29.5	28.2	
Fe <sub>2</sub> O <sub>3</sub>	2.65	2.65	2.66	2.67	
CaO	0.46	0.47	0.47	0.48	
Mg0	0.36	0.35	0.29	0.24	
TiO <sub>2</sub>	1.33	1.32	1.31	1.28	
Na <sub>2</sub> O	0.14	0.14	0.13	0.10	
K <sub>2</sub> O	0.79	0.79	0.76	0.13	
Other elements	2.67	2.48	1.88	0.90	
LOI	2.6	2.6	2.0	1.85	

**Table 2** Chemical composition of TAFA at different temperature determined by XRF technique.

Chemical	TAFA					
components	500 °C/2h	700 °C/2h	900°C/2h	900°C/4h		
SiO <sub>2</sub>	66	67	69	70		
$Al_2O_3$	29.8	29.8	29.9	29.9		
$Fe_2O_3$	1.02	0.56	0.29	0.01		
CaO	0.38	0.21	0.03	0.01		
MgO	0.18	0.12	0.08	0.01		
TiO <sub>2</sub>	0.23	0.11	0.05	0.02		
Na <sub>2</sub> O	0.11	0.10	0.04	0.01		
K <sub>2</sub> O	0.81	0.75	0.34	0.02		
Other elements	1.56	1.26	0.18	0.02		
LOI	1.01	0.5	0.4	0.08		

### 3.2 Structural Properties

The changes in the crystalline phases in FA after ball milling have been monitored with the help of wide angle X-Ray Diffraction studies. The broad gibbosity in XRD patterns in the range  $2\theta$  is between  $15^{\circ}\text{-}35^{\circ}$ , indicating the coexistence of amorphous components, which increases after mechanical activation, but decreases after thermal activation of fly ash. As compared with FA, the crystallite size is reduced as milling time was increase up to 15h but the crystallinity and crystallite size of thermally activated fly ash is higher than that of samples before activation due to increases in the crystalline phases.

The X-Ray diffraction patterns of the fresh as well as ball milled fly ash are given in the Fig. 1. A steady decrease in the crystallite size is observed and the quartz phase suffers the most. The same effect can be seen in the variation of peak height with milling time [19]. The peaks at  $16.4^{\circ}$ ,  $42.2^{\circ}$  and  $26.2^{\circ}$  show mullite (alumino silicate) phases while quartz (silica) exhibits strong peaks at  $20.7^{\circ}$ ,  $26.5^{\circ}$ ,  $26.66^{\circ}$ ,  $40.66^{\circ}$ ,  $49.96^{\circ}$  and  $54.2^{\circ}$  of  $20^{\circ}$  values. Peak at  $33.56^{\circ}$  and  $35.62^{\circ}$  indicate iron oxide phases [20, 21]. The 15h ball milling decreases the crystallinity of the fly ash, thus increases the amorphous domains in it. The peak intensity of quartz phase is reduced with increases in the milling hours (5h-15h).

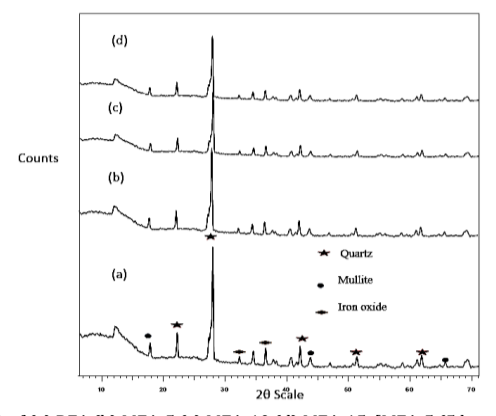


Fig. 1 XRD of (a) RFA (b) MFA-5 (c) MFA-10 (d) MFA-15. [MFA-5 (5 hr milled fly ash); MFA-10 (10 hr milled fly ash); MFA-15 (15hr milled fly ash)]

During thermal treatment of fly ash, quartz is inherited and crystallization of mullite and corundum occurs. Thermal treatment increases the crystalline nature of the ash thus decreases the amorphous nature, the crystallinity and crystallite size of quartz present in thermally activated fly ash is increased with increase in temperature of calcination. The formation of magnetite is more pronounced at high temperature activation than the other fly ash samples (FA and MFA). With thermal activation magnetite peak tends to disappear while a peak responsible for hematite begins to appear. XRD patterns of thermally activated fly ash samples calcined at different temperatures and durations are shown in Fig. 2.

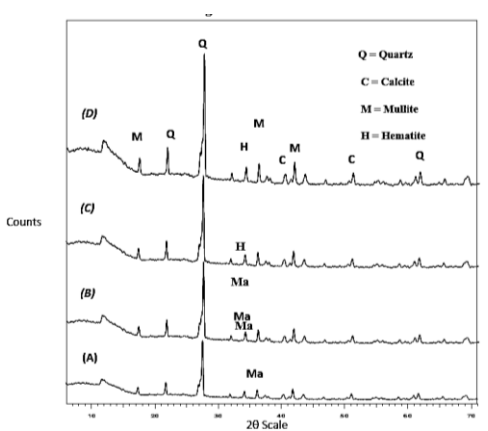


Fig. 2 XRD of (A) TAFA-500 °C/2h, (B) TAFA-700 °C/2h, (C) TAFA- 900 °C/2h and D) TAFA-900 °C/4h.

Thermal treatment decreases the carbon content of fly ash and moisture from mineral phases resulting in change in colour [22]. The results are presented in Table 3. A lighter colour results from heating to 500 °C is due to oxidation of carbon. A colour change between 700 °C and 900 °C corresponds to the crystallization of phases stabilized as the glass content is reduced. The loss on ignition (LOI) increases from 500 °C to 900 °C, between 700 °C and 900 °C the LOI data shows a region of relative stability. This result confirms that the thermal treatment of fly ash indicates change in color, LOI and phase mineralogy. The mineralogical changes are more pronounced above 500 °C.

Table 3 LOI, colour and crystalline phase changes with temperature for fly ash

Temp °C/time	LOI	Colour	Magnatite	Hematite	Mullite	Quartz
900/4h	0.08	Yellowish brown		<b>✓</b>	✓	✓
900/2h	0.4	Light yellowish brown	✓	<b>√</b>	✓	✓
700/2h	0.5	Light yellowish brown	✓	✓	✓	✓
500/2h	1.01	Pale brown	✓	✓	✓	✓
Not heated	2.6	Grayish brown	✓		✓	✓

✓ - Indicates continued presence of crystalline phase Gray box - indicates slight change in intensity

# 3.3 FT-IR Studies

The FT-IR spectra of different FA, MFA and TAFA samples are given in Fig. 3 and Fig. 4, show a broad band between 3600-3000 cm<sup>-1</sup>, which is attributed to surface -OH groups of Si-OH and adsorbed water molecules on the surface. The broadness of the bond is due to the strong hydrogen bonding. A peak at 1608, 1613 and 1680 cm<sup>-1</sup> in the spectra of both inactivated and activated fly ash samples is attributed to bending mode  $(\delta_{O-H})$  of water molecule. Peaks at 1100 cm<sup>-1</sup> correspond to Si-O-Si asymmetric stretching vibrations [23].

The increment in broadness between 3600-3300 cm<sup>-1</sup> after ball milling at 5 to 15h is an evidence for the breaking down of the quartz structure and formation of Si-OH groups [9]. However, FT-IR studies clearly show changes in the broadening of IR peaks corresponding to Si-O-Si asymmetric stretching vibrations (1161 cm<sup>-1</sup>) indicating structural rearrangement during 15h mechanical milling. Comparison of FT-IR

spectra of FA and MFA shown in Fig. 3 which clearly show changes in the intensity of IR peaks corresponding to Si-O-Si symmetric stretching (697 cm $^{-1}$ ) and T-O-Si (T = Si, Al) asymmetric stretching (1161 cm $^{-1}$ ) after milling indicating structural rearrangement during mechanical activation.

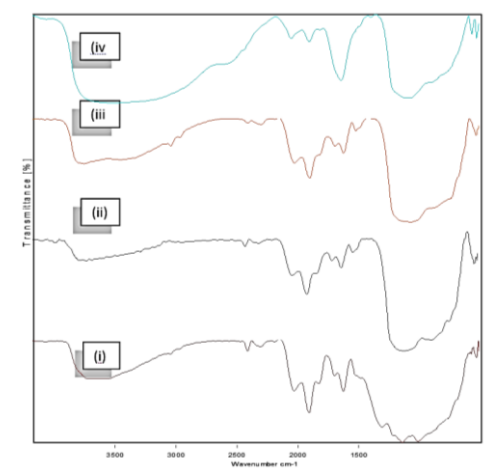


Fig. 3 FT-IR spectra of mechanically activated fly ash i) FA, (ii) MFA-5 (iii) MFA-10 and iv) MFA-15.

The FT-IR results of the thermally treated fly ash are shown in Fig. 4. The FT-IR spectra shows a broad band between 3500-3000 cm<sup>-1</sup>, which is attributed to surface -OH groups of silanol groups (-Si-OH) and adsorbed water molecules on the surface. The broadness of band indicates the presence of strong hydrogen bonding [24]. The gradual decrement in the intensity and broadness in this band, as shown in Fig. 4 confirms loss of water in all thermally treated samples during thermal activation. Most of the molecular water gets removed from the sample by heating up to 250 °C, while crystalline -OH remains in the sample till 700 °C [25]. A peak around 1682 cm $^{\text{-}1}$  is attributed to bending mode ( $\delta \text{O-H}$ ) of water molecule [26] which is shown in all fly ash samples. A broad band ranging from 1070 cm<sup>-1</sup> to 1170 cm<sup>-1</sup> due to Si-O-Si asymmetric stretching vibrations [27] of silica is present in fly ash. FA shows Si-O-Si asymmetric stretching vibration centered at 1100 cm<sup>-1</sup> which get shifted towards higher wave number at 1162 cm<sup>-1</sup> in case of TAFA-900 °C. This high wave number shift is the result of loss of water [28]. Peaks appear around 2343 cm-1 attributed to v O-H stretching [29], 2241 cm<sup>-1</sup> responsible for H-SiO<sub>3</sub> [30], 1984 cm<sup>-1</sup> due to =Si-H monohydride [31], 1872 cm<sup>-1</sup> due to calcium carbonate [32] present in all fly ash samples. Peaks associated with mullite appear at around 515 cm<sup>-1</sup>. Both the peaks are present in original fly ash as well as in the thermally treated fly ashes but the bands associated with silica tetrahedral and alumina tetrahedral, respectively at around 1152 and 820 cm<sup>-1</sup> are found when the sample was treated at 700 °C and 900 °C. At 900°C, mullite gives sharp peak due to the well-crystalline mullite. With the increase in the heating temperature, % transmission of the IR radiation increased.

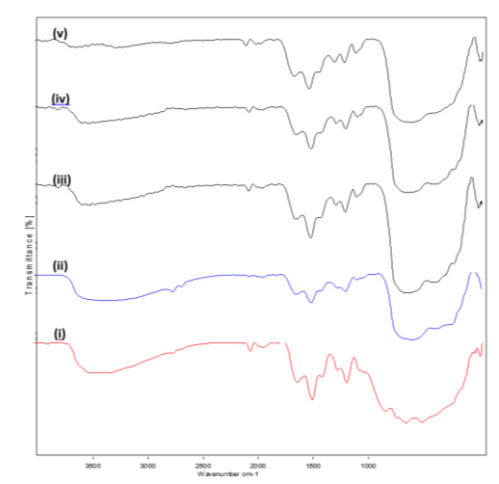


Fig. 4 FT-IR spectra of thermally activated fly ash (i) FA (ii) TAFA-500 °C/2h, (iii) TAFA-700 °C/2h, (iv) TAFA-900 °C/2h and (v) TAFA-900 °C/4h.

## 4.4 SEM Analysis

The SEM images of FA, MFA and TAFA samples are shown in Figs. 5 to 7. The investigation reveals that most of the particles present in the FA

samples are spherical in shape with relatively smooth surface consisting of quartz, clusters of iron particles formed due to partial decomposition of pyrite and dark quartz inclusions [33]. The typical SEM images of mechanically activated fly ash samples show the structural changes of larger particles and increased surface roughness which is increased with increase in milling time 5 to 15h (Fig. 6). The smooth spherical cenospheres are affected most resulting remarkable changes in morphology and breaking of spherical silica structure. After thermal activation of fly ash sample at different temperature char and carbonaceous materials are removed by calcinations which is also revealed from the SEM images of fly ash after thermal activation (Fig. 7). The decrease might be because of the increase in the spheroid nature of the magnetic particles formed from the transformation of some hematite phases into magnetite.

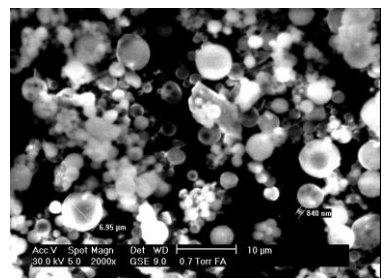


Fig. 5 SEM micrograph of pure fly ash (FA).

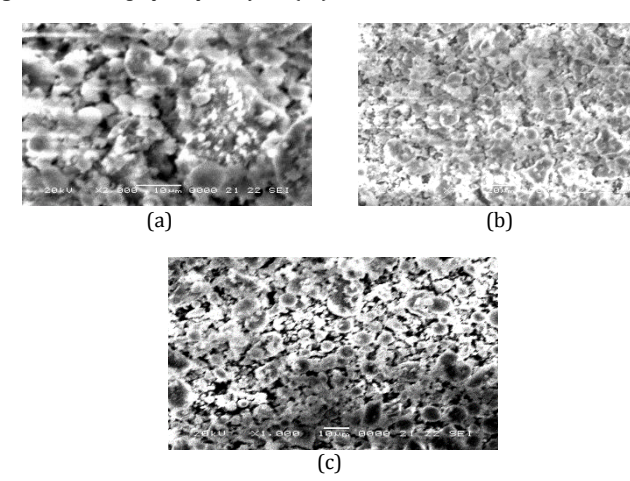


Fig. 6 SEM micrographs of (a) MFA-5h, (b) MFA-10h and (c) MFA-15h.

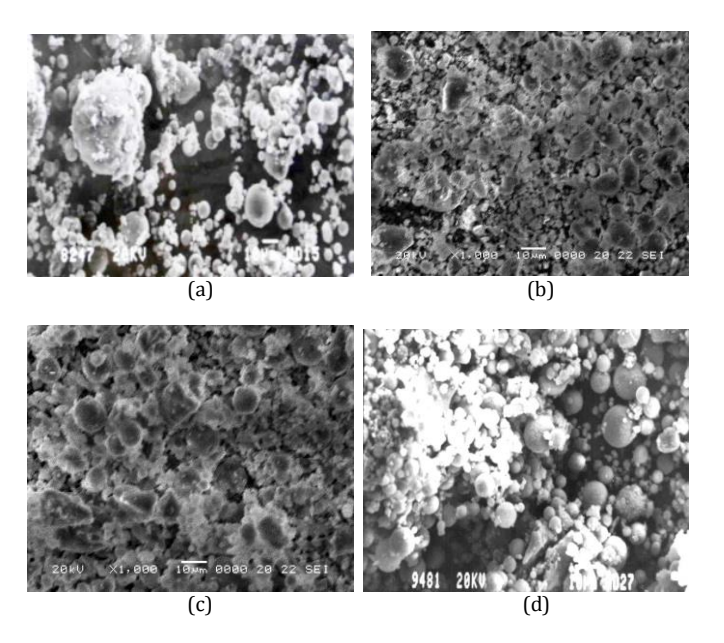


Fig. 7 SEM micrographs of (A) TAFA-500 °C/2h, (B) TAFA-700 °C/2h, (C) TAFA-900 °C/2h and (D) TAFA-900 °C/4h.

The mechanical and thermal activation of fly ash affects its surface properties. The variation in BET surface area of FA with different milling time and temperature is shown in Table 4 which indicates that the BET surface area is increased marginally after milling for 5 to 15h and increased from 0.97 m²/g to 2.57 m²/g, which is further increased to 2.99 m²/g after thermal activation [20]. This result confirms that the thermally treated fly ash has a higher specific surface area of 2.99 m²/g than the mechanically activated (15h) fly ash with 2.57 m²/g [9, 34].

Table 4 Characterization of fly ash before and after activation

		MFA			TAFA			
Samples	FA	MFA 5h	MFA 10h	MFA 15h	TAFA 500°C /2h	TAFA 700°C /2h	TAFA 900°C /2h	TAFA 900°C /4h
BET surface area (m <sup>2</sup> /g)	0.97	1.88	2.46	2.57	2.65	2.72	2.85	2.99

## 3.5 TGA-DTA Analysis

Fig. 8 shows the TG-DTA curves of the coal fly ash. The DTA curve shows three exothermic peaks at 580 °C, 700 °C and 950 °C during the heating process, while no exothermic peak is observed during the cooling process. Thus, the exothermic peaks are attributable to an irreversible reaction. The TG curve began to decrease at 580 °C and reached a steady state at over 950 °C [35, 36]. It is speculated that the exothermic peak at 580 °C in air was due to combustion of the unburned carbon in the coal fly ash, which led to a mass decrease. The exothermic peaks at 700 and 950 °C could have resulted from evaporation of Na<sub>2</sub>O and K<sub>2</sub>O alkali oxides of low melting point and crystallization of the glass phase.

TGA and DTA analysis curves of MFA (15h milling) are shown in Fig. 9 which indicates that there are three important changes (i) the first is a loss of weight between room temperature and 100 °C related to the loss of humidity, (ii) then from 100 to 450 °C, hydration water is lost, (iii) between 450 °C and 700 °C, there is a further loss of weight attributed mainly to the decomposition of CaCO $_3$  and the burning of residual coal present in the fly ash. Differential thermal analysis shows an additional change above 900 °C [37,38]. It is interesting to get different TGA and DTA curves for mechanically activated fly ash from raw fly ash, which also confirms that there are same morphological changes in mineral phases during milling.

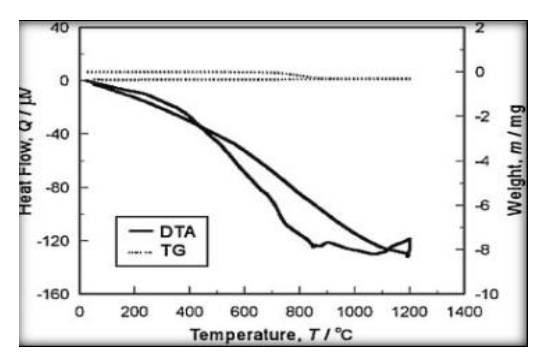


Fig. 8 TGA-DTA curves of fly ash

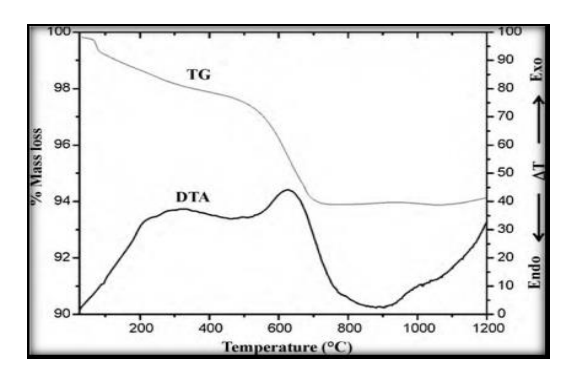


Fig. 9 Differential and gravimetric thermal analysis of MFA

#### 4. Conclusion

Fly ash contains high silica content, which helps in converting it as an active catalytic material like other silica sources. After suitable activation and modified surface activity, FA can be converted as an active catalytic support for synthesis of heterogeneous catalyst for various organic transformations. The mechanical activation of fly ash using high energy

ball mill affects the surface properties of the fly ash more than the other properties. FA can be transformed from micron sized to nano structured through high energy planetary ball milling. Such mechanical activation not only improves degree of fineness but also involves breaking of bonds, dispersion of solids, generation and migration of chemical moieties in the bulk thus results in increased surface roughness and specific surface area. Transformation of quartz and cristobalite phases into a glassy phase is also faster in MFA. With increase in milling duration from 5h to 15h silica percentage is marginally changed whereas the crystallite size of crystalline phase is reduced and specific surface area is increased from 1.88 to 2.57 m<sup>2</sup>/g. Due to thermal activation the mullite content is increased, some of the magnetite phases are convert into hametide phases, activated carbon and sulphur content are reduced. It is concluded that the modification properties of FA can be achieved by mechanical and thermal activation methods to generate degree of reactivity on FA in the form of surface silanol groups as a catalyst or catalyst support material. It is concluded that the mechno-thermal activation can generate sufficient activity on fly ash surface rendering its potential application in heterogeneous catalysis.

#### Acknowledgement

The authors are thankful to Dr. D.D. Phase and Er. V.K. Ahiray for SEM-EDX analysis and Mukul Gupta for XRD conducted at UGC DAE-CSR Lab Indore. XRF analysis was conducted at Punjab University, Chandigarh. The financial support was provided by Fly Ash Mission, Department of Science and Technology, New Delhi, India.

#### References

- Anonymous, The Italian approach to the problem of fly ash, Paper 84, International Ash utilization symposium, Center for applied Energy Research, University of Kentucky, USA, 1999.
- [2] Z.T. Yao, M.S. Xia, Y. Ye, Synthesis of zeolite Li-ABW from fly ash by fusion method, J. Hazard. Mater. 170 (2) (2009) 639-644.
- [3] S. Katara, A. Sharma, S. Kabra and A. Rani, Surface modification of fly ash by thermal activation: A DR/FTIR study, Int. Res. J. Pure Appl. Chem. 3(4) (2013) 299-307.
- [4] M. Kobya. V.S. Drozhzhin, M.Ya. Shpirt, L.D. Danilin, Formation processes and main properties of hollow aluminosilicate microspheres in fly ash from thermal power stations, Solid Fuel Chem. 42 (2008) 107-119.
- [5] B.G. Kutchko, A.G. Kim, Fly ash characterization by SEM-EDS, Fuel 85 (2006) 2537-2544.
- [6] O. Dogen, M. Kobya, Elemental analysis of trace elements in fly ash samples of yatagan thermal power plants using EDXRF, J. Quant. Spectro. Rediat. Trans. 101 (2006) 146-150.
- [7] M. Fan, R.C. Brown, Comparison of the loss on ignition and thermo-gravimetric analysis techniques in measuring unburned carbon in coal fly ash, Energy Fuels 15 (2001) 1414-1417.
- [8] R. Kumar, S. Kumar, S.P. Mehrotr, Towards sustainable solutions for fly ash through mechanical activation, Resour. Conserv. Recyc. 52 (2007) 157-179.
- [9] J. Rao, P. Narayanaswami, S. Prasad, Thermal stability of nano structured fly ash synthesized by high energy ball milling, Int. J. Eng. Sci. Technol. 2 (5) (2010) 284-299
- [10] P. Arjunan, Fly ash India 2005, Ash Symposium 2005, International conference 'World of coal Ash 2005'; 20-25 (http://whocares.caer.uky.edu/wasp/Ash Symposium - Accessed on 15 Feb 2015).
   [11] F. Rongli, A. Palomo, M.T. Blanco, M.L. Granizo, F. Puertas, T. Vazquez, M.W.
- [11] F. Rongli, A. Palomo, M.T. Blanco, M.L. Granizo, F. Puertas, T. Vazquez, M.W. Grutzeck, Chemical stability of cementitious materials based on metakaolin, Cem Concr Res 29(1999) 997–1004.
- [12] W. Bao-min, W. Li-jiu, Development of studies and applications of activation techniques of fly ash, PRC International Workshop on Sustainable Development and Concrete Technology, School of Civil Engineering, Dalian University of Technology, Dalian, 116024, 2004, pp. 159-169.

- [13] G. Kovalchuk, Alkali-activated fly ash: Effect of thermal curing conditions on mechanical and microstructural development -Part II, Fuel 86 (2007) 315-322.
- [14] J. Marrero, Characterization and determination of 28 elements in fly ashes collected in a thermal power plant in Argentina using different instrumental techniques, Spectrochemi. Acta Part B 62 (2007) 101-108.
- [15] B.D. Cullity, S.R. Stock, Upper Saddle River, 3rd Edn., NJ: Prentice Hall, CITY/COUNTRY, 2001, p. 388.
- [16] A. Sharma, A. Rani, Modification in chemical, structural and morphological properties of fly ash through mechanical activation, Int. J. Curr. Res. 7 (02) (2015) 12828-12834.
- [17] K.T. Paul, S.K. Satpathy, I. Manna, K.K. Chakraborty, G.B. Nando, Preparation and characterization of nano structured materials from fly ash: A waste from thermal power stations by high energy ball milling, Nanoscale Res. Lett. 2 (2007) 397-404.
- [18] L.L. Shaw, R. Ren, Z. Ban, Z. Yang, Thermomechanical Properties of Wet Shotcrete Refractory Castable Matrices, Ame. Ceram. Soc. 137 (2003) 50-69.
- [19] P.J. Willians, J.J. Biernacki, C.J. Rawn, L. Walker, J. Bai, Microanalytical and Computational Analysis of a Class F Fly Ash, ACI Mater. J. 102 (5) (2005) 330.
- [20] A. Sharma, K. Srivastava, V. Devra, A. Rani, Modification in properties of fly ashthrough mechanical and chemical activation, Amer. Chem. Sci. J. 2(4) (2012) 177-187.
- [21] J.M. Fox, World of coal ash (WOCA), April 11-15, Lexington, Kentucky, USA, 2005.
- [22] G.A. Patil, S. Anandhan, Ball milling of class-F Indian fly ash obtained from a thermal power station, Int. J. Energy Eng. 2 (2012) 57-62.
- [23] C. Khatri, A. Rani, Synthesis of nano-crystalline solid acid catalyst from fly ash and its catalytic performance, Fuel. 87(13) (2008) 2886-2892.
- [24] I.G. Richardson, The calcium silicate hydrates, Cem. Concr. Res. 38 (2008) 137-158.
- [25] A. Palomo, M.W. Grutzeck, M.T. Blanco, Alkali-activated fly ashes: A cement for the future, Cem. Concr. Res. 29 (1999) 1323-1329.
- [26] B.J. Saikia, G. Parthasarthy, N.C. Sarmah, G.D. Baruah, Fourier-transform infrared spectroscopic characterization of naturally occurring glassy fulgurites, Bull Mater. Sci. 31 (2) (2008) 155-158.
- [27] E.S. Morten, S. Camilla, Z.Li, E.G. Sogaard, XPS and FT-IR investigation of silicate polymers, J. Mater. Sci. 44 (2009) 2079-2088.
- [28] M.I. Zaki, H. Knozinger, B. Teshe, G.A.H. Mekhemer, Influence of phosphonation and phosphation on surface acid-base and morphological properties of CaO as investigated by in situ FTIR spectroscopy and electron microscopy, J. Colloid. Interface. Sci. 303 (2006) 9-17.
- [29] X.H. Sun, S.D. Wang, N.B. Wong, D.D. Ma, S.T. Lee, B.K. Teo, Silicon nanowires terminated with methyl functionalities exhibit stronger Si–C bonds than equivalent 2D surfaces, Inorg. Chem. 42 (2003) 2398-2404.
- [30] M. Blanco, P. Garcia, J. Ayala, Variation in fly ash properties with milling and acid leaching, Fuel 84 (2005) 89-96.
- 31] Jacox, E. Marilyn, Vibrational and electronic energy levels of polyatomic transient molecules, Supplement B, J. Phys. Chem. Ref. Data 32 (1) (2003) 1-5.
- [32] L. Offler, E. Lohse, U. Peuker, C. Oehlmann, L.M. Kustov, V.L. ZholObenko, The dehydroxylation of the kaolinite clay minerals using infrared emission spectroscopy, Clays and Clay Miner. 44 (1996) 635-651.
- [33] M.A. Legodi, D. DeWaal, J.H. Potgieter, S.S. Potgieter, Rapid determination of CaCO3 in mixtures utilising FT-IR spectroscopy, Miner. Eng. 14 (2001) 1107-1111.
- [34] K. Hasezaki, A. Nakashita, G. Kaneko, H. Kakuda, Unburned Carbon Behavior in Sintered Coal Fly-Ash Bulk Material by Spark Plasma Sintering, Mater. Trans. 48 (12) (2007) 3062-3065.
- [35] M. Versan Kok, An investigation into the thermal behavior of coals, Energy Sources 24 (10) (2002) 899-905
- [36] G. Stefanovi, L. Ojba, I. Sekuli, S. Matija, Hydration study of mechanically activated mixtures of Portland cement and fly ash, J. Serb. Chem. Soc. 72 (6) (2007) 591-604.
- [37] X. Nie, W.H. McClennen, K. Liu, H.L.C. Meuzelaar, Development of on-line GUMS monitoring techniques for high pressure fuel conversion processes, ACS Fuel Chem. Div. Preprints 38 (4) (1993) 1147-1159.
- [38] K. Liu, E. Jakab, W.H. McCkMen, H.L.C. Meuzelaar, Fourier-transform infra applications of the thermogravimetric analysis in the study of fossil fuels, ACS Fuel Chem. Div. Preprints 38 (3) (1993) 823-842.